平成 23 年度

三重大学　大学院生物資源学研究科

修士論文

The Relationship between the Arctic Sea-ice Recovery and Atmospheric Circulations in Autumn

秋季における北極海の海氷回復と大気循環の関係

Climate and Ecosystems Dynamics Division
Graduate school of Bioresources
Mie University

510M227　Masashi Ito
Supervisor: Prof. Yoshihiro Tachibana

27 February 2012

Abstract

As the sea-ice extent decreases during summer over the Arctic, it tends to recover quickly during autumn. I investigated a relationship between the sea-ice recovery and atmospheric circulations over the Arctic in the beginning of freezing season. The object domain is the Pacific sector (70°-90°N, 270°-90°E) in the Arctic Ocean. I analyzed the sea-ice growth rates per day each month (Sep. Oct. Nov.) and the conditions of atmospheric pressure patterns when the sea-ice is generated in autumn from 1979-2010 with ERA-Interim.reanalysis data. The sea-ice growth rates tend to increase recent years. The sea surface atmosphere cold temperature is important for the sea-ice generation. In addition, a cyclone or an anticyclone needs to be located at the cold temperature area. Because the cyclones exist on sea-ice with cold advection to the Arctic ice edge, the upward heat flux from the Arctic Ocean activates the freezing the sea ice. Therefore, the cold air of the lower troposphere and circulations with cyclones or anticyclones on the cold air is needed to generate the sea-ice. Recently, the pressure pattern has changed. The rate of sea-ice generation has increased on October, because signature pressure pattern occurs rather than few decades ago. Additionally, the decreasing horizontal temperature flux roles cooling the Arctic. Both factors affect the much sea-ice generation recent years.

1. Introduction

1.1 Decreasing of sea-ice in the Arctic Ocean

The Climate has been dramatically changing in recently years. Especially, the Arctic lower troposphere has been warming more than twice as fast as the global average over the past century (Figure.1) [*Intergovernmental Panel on Climate Change*, 2007; *Screen and Simmonds*, 2010]. The Arctic sea-ice extent in summer season was recorded minimum value in 2007 [*Stroeve et al.,* 2008]. An accelerating retreat of the Arctic sea-ice in recent decades, evident in all months of the year, is one of the most dramatic signals of global climate change worldwide. The sea-ice loss relates to atmospheric circulation. Key factors behind this ice loss include thinning of the pack ice in recent decades coupled with an unusual pattern of atmospheric circulation [*Nghiem et al*., 2007; *Maslanik et al*., 2007]. Shimada et al., (2006) showed that decreasing of the Sea-ice and thinning of the Sea-ice leads to increase fluidity of the Sea-ice, and it get Sea-ice decreasing dynamically. Furthermore, the atmospheric circulation with unusual continuous anticyclonic circulation on Beaufort Sea drifts the sea-ice from the Arctic sea to the Atlantic Ocean, and it causes additional sea-ice loss (Figure.2) [*Ogi and Wallace,* 2007]. Overall, due to increasing of the open water area, ice-albedo feedback is promoted [*Morits et al*., 1993; *Perovich et al*., 1999; *Uttal et al.*, 2002; *Inoue et al*., 2005]. As a result, such sea-ice loss will likely influence mid-latitude patterns of atmospheric circulation and precipitation [e.g., *Sewall and Sloan*, 2004], because the sea-ice loss changes the condition over the Arctic Ocean.

1.2 Increasing of sea-ice in the Arctic Ocean

The influence which occurred in summer continues until fall. In terms of heat budget, heat which stocked in the Arctic sea in summer comes out from the Arctic sea in fall (Figure.3) [*Screen and Simmonds*, 2010]. Thus, due to the increasing of open water and decreasing of the sea-ice, the melt season has been longer [*Perovich et al.,*2006]. In this way, due to the influence in summer affects the sea-ice and atmospheric circulations in fall and the condition of sea-ice in fall affects next summer sea-ice, we must consider not just decreasing of sea-ice but increasing one for understanding a set of the sea-ice change. In fact, *Stroeve et al.*, (2007) shows that the amount of sea-ice reduction over the past few decades exceeds the forecast of IPCC AR4 (Intergovernmental Panel on Climate Change Fourth Assessment Report) (Figure.4). For generation of the sea-ice, the atmospheric circulations also play an important role when the sea-ice is generated. At the beginning of fall, when a cyclone moves toward the north from sea area without sea-ice to sea-ice area, it gets energy from ocean and develops. And, it triggers cooler fluid and freezes the sea. It appears that frontal cyclogenesis during autumn works as an accelerator of heat exchanges between the atmosphere and the ocean [*Inoue and Hori*, 2011]. It showed that the atmosphere related to the generation of the sea-ice. It is important considering the heat budget when the sea-ice is generated. From autumn into winter, the atmosphere cools in response to the declining solar flux. However, the net surface flux turns positive largely because of sea–ice growth and sensible heat loss from the ocean [*Nakamura and Oort*, 1988, *Serrezze et al*., 2007].

1.3 Theme

The sea-ice has decreased in summer, and the sea-ice growing rate has increased with short freezing season in autumn [*Bitz and Roe*, 2004]. For freeze onset, Inoue and Hori, (2011) shows that relationship between a cyclone and the sea-ice generation. But, what trigger become for releasing heat from the sea to atmosphere. It is uncertain what situations do generate the sea-ice in the Arctic Ocean. This paper shows the relationship between the Arctic sea-ice recovery and atmospheric circulations in terms of heats and pressure patterns with daily data during freezing season, 1979-2010.

2. Data and Methods

2.1 Sea-ice concentration

Daily sea-ice concentrations (SIC) on a 25km×25km grid for the period August – December from 1979 to 2010 were obtained from the National Snow and Ice Data Center (NSIDC) in Boulder, Colorado. These data are derived from the Nimbus-7 Scanning Multichannel Microwave Radiometer (SMMR) and Defence Meteorological Satellite Program (DMSP) –F8, –F11 and –F13 Special Sensor Microwave/Imager (SSM/I) radiances using the NASA team algorithm [*Cavalieri et al.,* 1999]. I defined the object domain area as the Pacific sector (70°-90°N, 90°-270°E) in Figure.5. And, I also defined the Pacific sector ice extent index (PSI) as the area mean ice concentration within the area.

2.2 ERA-Interim reanalysis data

I also make use of, mean sea level pressure (MSLP), surface latent heat flux (SLHF), surface sensible heat flux (SSHF), sea ice concentration (SIC), surface air temperature, surface wind data from the European Center for Medium Range Weather Forecasts (ECMWF) Interim re-analysis (ERA-Interim) [*Dee and Uppala,* 2009]. The resolution is 1.5° ×1.5 ° for the period August – December from 1979 to 2010.

2.3 Sea-ice and pressure pattern

In order to investigate the condition of sea-ice each year when the value is recorded minimum, I analyzed the PSI time series which values is minimum each year (Figure.6), and that's date (Figure.7). In order to investigate the recovery of sea-ice in freezing season each year, I analyzed the PSI time series at 1st each month (Oct. Nov. Dec.) (Figure.8). Figure.9 shows time series of increment of area-averaged sea-ice concentration per day on Oct. and Nov. from 1979 to 2010. This means that when the sea-ice recover. The

condition of sea-ice in summer relate to that in winter. In a similar way, I investigated the relationship between the sea-ice concentration at 1st on each month (Oct. and Nov.) and the recovery rate of the sea-ice concentration each month (Figure.10). Finally, I selected the turning point in which the ice begins to continuously increase in each year. These 32 pressure patterns are classified into 3 groups roughly (Figure.11).

2.4 Composite analysis

I analyzed the composite of SLP for identifying the characteristics of pressure pattern when the sea-ice is generated. I used the SLP and growth rate of sea-ice. They are chosen from the growth rate in the top 5years of 32years. Finally, I show a correlation between index SLP composite anomaly and sea-ice growth rate on October.

3. Results

3.1 Sea-ice concentration in the Pacific sector

Figure.6 shows the minimum value of the sea-ice concentration in the Pacific sector from 1979 to 2010 when the value is recorded minimum one. The minimum value tends to decrease and the decreasing rate is about 10% per decade since 1979. This sea-ice loss in the Pacific sector is caused by thinning of the pack ice [*Nghiem et al*., 2007] and atmospheric circulation [*Ogi and Wallace,* 2007] etc. Due to the sea-ice loss, the melting season tends to longer [*Perovich et al.*,2006]. Based on this, 30 years ago the minimum day is the end of August, however, the minimum value day is mid-September recently. And, the minimum value day tends to delay gradually (Figure.7). I analyzed PSI at first day each month (Oct. Nov. Dec.) since 1979 (Figure. 8). This shows that the values on October decrease. But, on November and December, the values remain roughly flat. This means that the sea-ice recovery occurs on October. Therefore, I analyzed the sea-ice recovery rate per day on October and November (Figure. 9). The rate on October is much bigger than November. That value decreases and ability of recovery is twice of 30 years ago. Despite delay of minimum day, recovery rate increases. Thus, most of recovery occurs on October. Additionally, I found that the recovery rate relates to the sea-ice concentration in summer season (Figure.10). This figure shows a clear inverse correlation between the sea-ice concentration on October 1st and the recovery rate per day on October since 1979. This means that no matter how the sea-ice decreases in melting season, it certainly recovers mostly on October in the Pacific sector. Recently, the amount of the sea-ice recovery increases with the sea-ice loss in summer. For this reason, I think that there are some key factors on October when the sea-ice recovers.

3.2 Sea-ice recovery and pressure patters

Figure.11a-c shows typical pressure patterns when the sea-ice is generated. I selected the turning point in which the growth rate of the area-averaged PSI (the region is the Pacific sector) begins to continuously increase over 1% from August to December each year. And, I defined the first day which last over 5 days as a turning point day. I chose 32 pressure patterns when the turning point day since 1979. These 32 pressure patterns are classified into three groups roughly. One of the three pressure patterns is a dipole pattern: a low-pressure system and a high-pressure system are located in pairs around North Pole (Figure.11a). Another is a single low-pressure system pattern: a low-pressure system is located over the Laptev Sea or the East Siberian Sea (Figure.11b). The other is a single high-pressure system pattern: a high-pressure system is located around North Pole. In the dipole pattern, sea-ice increases between the low-pressure system and the high-pressure system (Figure.11c). In the single low-pressure system pattern and the high-pressure system pattern, sea-ice increases right on them or around them. For the fig.11a, a high-pressure system which has an atmospheric pressure of 1028hPa at this center is located over the Laptev Sea or the East Siberian Sea and a low-pressure system which has an atmospheric pressure of 984hPa at this center is located over the Beaufort Sea. For the fig.11b, a low-pressure system which has an atmospheric pressure of 988hPa at this center is located over the Laptev Sea. For the fig.11c, a high-pressure system which has an atmospheric pressure of 1020hPa at this center is located over the Laptev Sea and the East Siberian Sea. Therefore, the pressure pattern is not only one and severely dispersed. Thus, I need to identify the characteristics of pressure patterns when the sea-ice generated.

3.3 Composite analysis about SLP and sea-ice growth

In order to identify the characteristics of pressure patterns when the sea-ice is generated, I did composite analysis. Figure.12a-b shows SLP composite. (a) shows the SLP composite when the recovery rate of sea-ice per day is over 1% and (b) shows it when that is over 2%. SLP anomaly of (b) is more clearly than (a). It means that sea-ice recovery may occur when the contrast of low pressure and high pressure is clear. Furthermore, Figure.13 shows SLP composite anomalies. This is anomaly from the mean on October since 1979. This also (b) is more clearly than (a). For pressure systems, figure.12 shows that the negative area locates from south Alaska to Okhotsk. The positive area locates around the Arctic pole and mid-latitude. Figure.13 shows that the negative area locates from mid-Siberia to northern America. The positive area locates in Europe, the Atlantic Ocean and around the Arctic pole. When the sea-ice is generated, negative area tends to locate in the Arctic sea area, comparatively. Thus, on the Arctic Ocean combination of positive area and negative area is clear. In these times, the sea-ice growth has a pronounced tendency to increase in East Siberian Sea (Figure. 14a.b). These high growth rate areas locate on the high pressure gradient area between positive composite value and negative one. Furthermore, negative climate value of SLP (Figure.15) corresponds to negative composite value, and vice versa. When the sea-ice is generated, the negative pressure area becomes less negative and the plus pressure area becomes more positive. Thus, in this time, pressure gradient on the Pacific area get stronger.

3.4 The trend of SLP on October

The trend of SLP on October from 1979 to 2010 tends to positive in center of Arctic and negative in the Aleutian and Siberia (Figure.16). This distribution resembles that of composite anomaly and climate value. This means that it gets the pressure lower in the low pressure area and stronger in the high pressure area. Due to this influence, because the pressure gradient gets bigger, winds in Arctic flow strongly when the sea-ice is generated.

3.5 Index of pattern correlation with SLP

Figure.17 shows that index of pattern correlation between SLP composite anomalies with daily SLP anomalies. In the mid 1990s the index value is small temporarily. But, the value shows high recently. Thus, in recently years, this SLP composite anomaly occurs rather than in the past. Additionally, figure.18 shows index of pattern correlation between SLP composite anomalies with daily SLP anomalies and index of increment of area-averaged (in the Pacific sector) sea-ice concentration per day on October. These trends have the increasing ones, respectively. These trends resemble each other. This correspondence of trends shows that the rapidly sea-ice generation occurs when daily SLP pattern correspond with the patter of SLP composite. Therefore, the pressure pattern relates to sea-ice generation. In fact, the correlation coefficient between this index of sea-ice growth rate and index of pattern correlation is 0.52.

3.6 Horizontal temperature flux

Figure.19 shows integration value of horizontal temperature flux. Integration objection is horizontal temperature flux which through the edge of Pacific sector. I defined the flux which way to this area as plus value. Horizontal temperature flux which comes into the Pacific sector tends to weaker recently. Thus, the heats comes into this area decreases on October. This means that decreasing of heat has a stimulating effect on heeling art temperature freezing and freezing sea-ice.

4 Discussion and Conclusions

The rapidly sea-ice recovery occurs on October. That's recovery rate is bigger than other months. Additionally, the recovery rate per day tends to increases, and this grows rapidly recently years. This pronounced recovery is in the coast of Siberia. In term of composite analysis, the distribution of SLP composite anomaly corresponds with the trend of SLP on October. Additionally, the trend of Index of pattern correlation between SLP composite anomalies with daily SLP anomaly corresponds to the trend of SLP on October. This means that the pattern like SLP composite anomaly tends to locate on the Arctic when the sea-ice is generated rapidly. Thus, pressure pattern with low pressure system and high pressure system tend to appear recently. Due to contrast of pressure pattern, wind flow strongly on this area. Thus, the cold advection comes to open water area. The cold air effects the heat comes out from sea to lower troposphere. After the heat loss, the sea-ice generates. Furthermore, horizontal temperature flux which comes into the Pacific sector tends to weaker recently. Thus, the heats comes into in this area decreases. This means that decreasing of heat has a stimulating effect on heeling air temperature freezing and freezing sea-ice. The correlation between index of sea-ice growth rate and index of pattern correlation is the highest value. On the other hand, the correlation between the temperature flux and pattern correlation is not good correlation. This is why the rapidly sea-ice generation occurs on October, nevertheless, the much heat stocks rather than few decades ago in open water during summer season.

5. Acknowledgement

I would like to express grateful thanks for Dr. Jun Inoue of JAMSTEC (Japan Agency for Marine-Earth Science and Technology) and Prof. Yoshihiro Tachibana, my supervisors, whose comments and suggestions were of inestimable value for my study. Therefore, I could never make it without their helps.

I would also like to grateful thanks for the members of Climate Dynamics Research Team of JAMSTEC and many scientists in other organizations whose meticulous comments were an enormous help to me.

I would also like to thank for Members of climate and ecosystems dynamics laboratory and course of geosystem science in factory of bioresources at Mie University who provide some advices for my research. In particular, laboratory's member always helped me in daily life. So, I enjoyed master's course for two years.

6. Reference

Bitz, C. M., and G. H. Roe , 2004: A mechanism for the high rate of sea ice thinning in the Arctic Ocean, *J. Clim.*, **17,** 3622–3632, doi:10.1175/ 1520-0442(2004)017<3623:AMFTHR>2.0.CO;2.

Inoue, J., T. Kikuchi, D.K. Perovich, and J.H. Morison, 2005: A drop in mid-summer shortwave radiation induced by changes in the ice-surface condition in the central Arctic. *Geophys. Res. Lett.*, **32**(13), L13603, doi:10.1029/2005GL023170.

Inoue, J., and M. Hori, 2011: Arctic cyclogenesis at the marginal ice zone: A contributory mechanism for the temperature amplification? *Geophys. Res. Lett.*, **38**, L12902, doi:10.1029/2011GL047696.

Intergovernmental Panel on Climate Change, 2007: *Climate Change 2007: The Physical Science Basis: Working Group I Contribution to the Fourth Assessment Report of the IPCC*, edited by S. Solomon et al., Cambridge Univ. Press, New York.

Maslanik, J. A., C. Fowler, J. Stroeve, S. Drobot, H. J. Zwally, D. Yi, and W. J. Emery (2007), A younger, thinner Arctic ice cover: Increased potential for rapid, extensives sea ice loss, *Geophys. Res. Lett.*, **34,** L24501, doi:10.1029/2007GL032043.

Moritz, R. E., J. A. Curry, A. S. Thorndike, and N. Untersteiner, 1993: SHEBA, a research program on the surface heat budget of the Arctic Ocean, *Rep.* **3**, 34 pp..

Nakamura, N., and A. H. Oort, 1988: Atmospheric heat budgets of the polar regions, J. Geophys. Res., **93**(D8), 9510－9524

Nghiem, S. V., I. G. Rigor, D. K. Perovich, P. Clemente- Colón, J. W. Weatherly, and G. Neumann, 2007: Rapid reduction of Arctic perennial sea ice, *Geophys. Res. Lett.,* **34**, L19504, doi:10.1029/2007GL031138.

Ogi.M, and J.M.Wallace, 2007: Summer minimum Arctic sea ice extent and the associated summer atmospheric circulation, *Geophys. Res. Lett.,* **34**, L12705, doi:10.1029/2007GL029897.

Perovich, D. K., et al., 1999: Year on ice gives climate insights, *Eos Trans. AGU*, **80**(41), 481, doi:10.1029/EO080i041p00481-01.

Perovich, D. K., S. V. Nghiem, T. Markus, and A. Schweiger, 2007: Seasonal evolution and interannual variability of the local solar energy absorbed by the Arctic sea ice–ocean system, *J. Geophys. Res.*, **112**, C03005, doi:10.1029/2006JC003558.

Screen, J. A., and I. Simmonds, 2010a: Increasing fall‐winter energy loss from the Arctic Ocean and its role in Arctic temperature amplification, *Geophys. Res. Lett.*, **37**, L16707, doi:10.1029/2010GL044136.

Screen, J. A., and I. Simmonds, 2010b: The central role of diminishing sea ice in recent Arctic temperature amplification, *Nature*, **464**, 1334–1337, doi:10.1038/nature09051.

Serreze, M. C., A. P. Barrett, A. G. Slater, M. Steele, J. Zhang, and K. E. Trenberth, 2007: The large-scale energy budget of the Arctic, *J. Geophys. Res.*, **112**, D11122, doi:10.1029/2006JD008230

Sewall, J. O., and L. C. Sloan, 2004: Disappearing Arctic sea ice reduces available water in the American west, *Geophys. Res. Lett.*, **31**, L06209, doi:10.1029/2003GL019133.

Uttal, T., et al., 2002: Surface heat budget of the Arctic Ocean, *Bull. Am. Meteorol. Soc.,* **83**, 255-275.

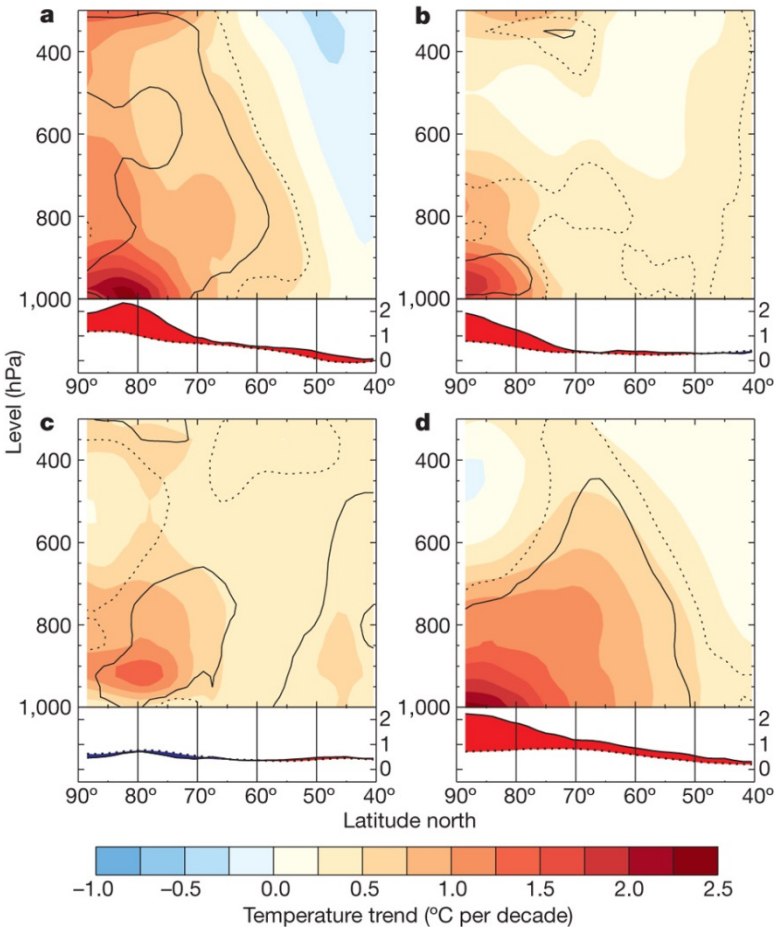

Figure.1 Temperature trends averaged around circles of latitude for winter (December–February; a), spring (March–May; b), summer (June–August; c) and autumn (September–November; d). The black contours indicate where trends differ significantly from zero at the 99% (solid lines) and 95% (dotted lines) confidence levels. The line graphs show trends (same units as in colour plots) averaged over the lower part of the atmosphere (950–1,000 hPa; solid lines) and over the entire atmospheric column (300–1,000 hPa; dotted lines). Red shading indicates that the lower atmosphere has warmed faster than the atmospheric column as whole. Blue shading indicates that the lower atmosphere has warmed slower than the atmospheric column as a whole.

(Screen and Simmonds., 2010)

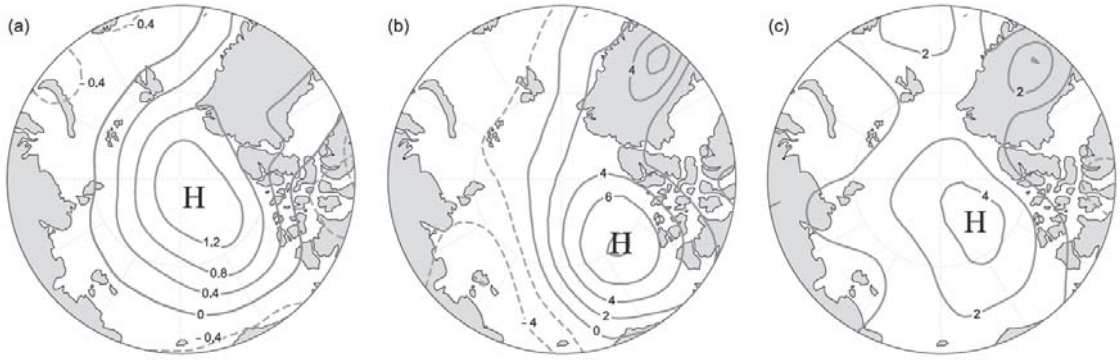

Figure.2　(a) Summer seasonal (July–August–September) mean SLP anomalies regressed on standardized index of May minus September sea ice extent over the Arctic basin as defined by the 15% ice concentration contour based on the period of record 1979–2006. (b) Summer seasonal (July–August–September) mean SLP anomalies for　2007. (c) Same as in Figure 3b but for 2008.

(Ogi et al., 2008)

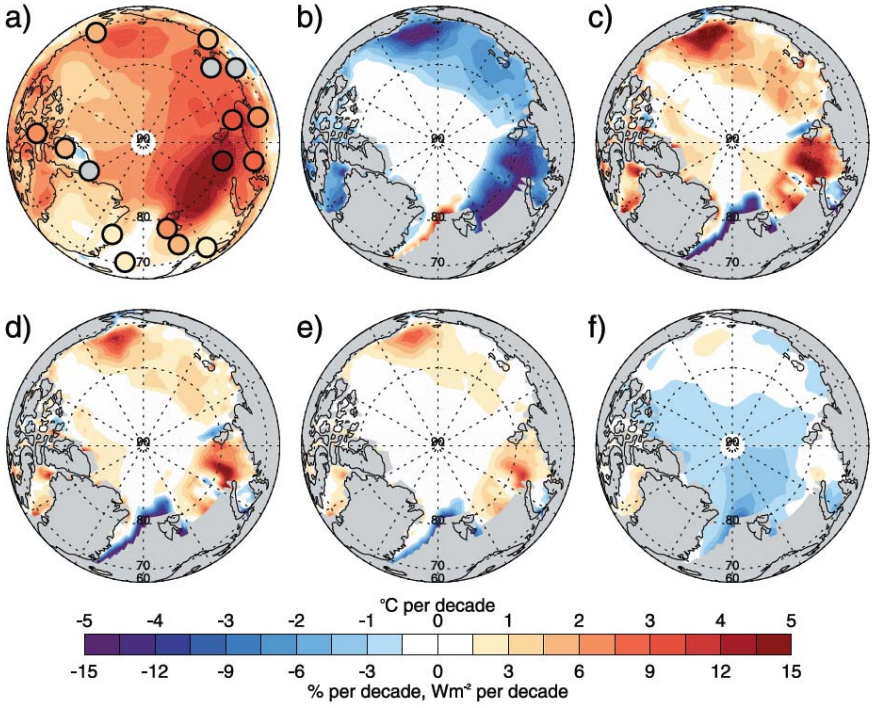

Figure.3 (a) Surface air temperature trends (°C per decade) during October–January, 1989–2009, from observations (colored dots) and from ERA‐Interim (shading). Gray dots indicate insufficient data was available to calculate the trends. The corresponding trends in ERA‐Interim for (b) sea ice concentration (% per decade), (c) surface turbulent heat fluxes (sensible plus latent), (d) surface sensible heat flux, (e) surface latent heat flux, and (f) net surface longwave radiation. The heat flux trends (Wm^{-2} per decade) are defined as positive in the upward direction.

(Screen and Simmonds., 2010a)

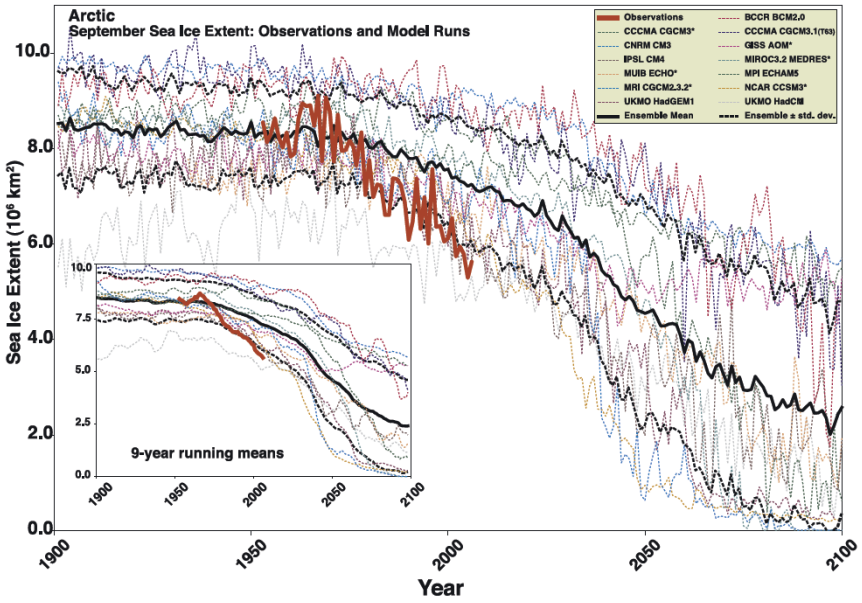

Figure.4 Arctic September sea ice extent ($\times 10^6$ km^2) from observations (thick red line) and 13 IPCC AR4 climate models, together with the multi-model ensemble mean (solid black line) and standard deviation (dotted black line). Models with more than one ensemble member are indicated with an asterisk. Inset shows 9-year running means.

(Stroeve et al., 2007)

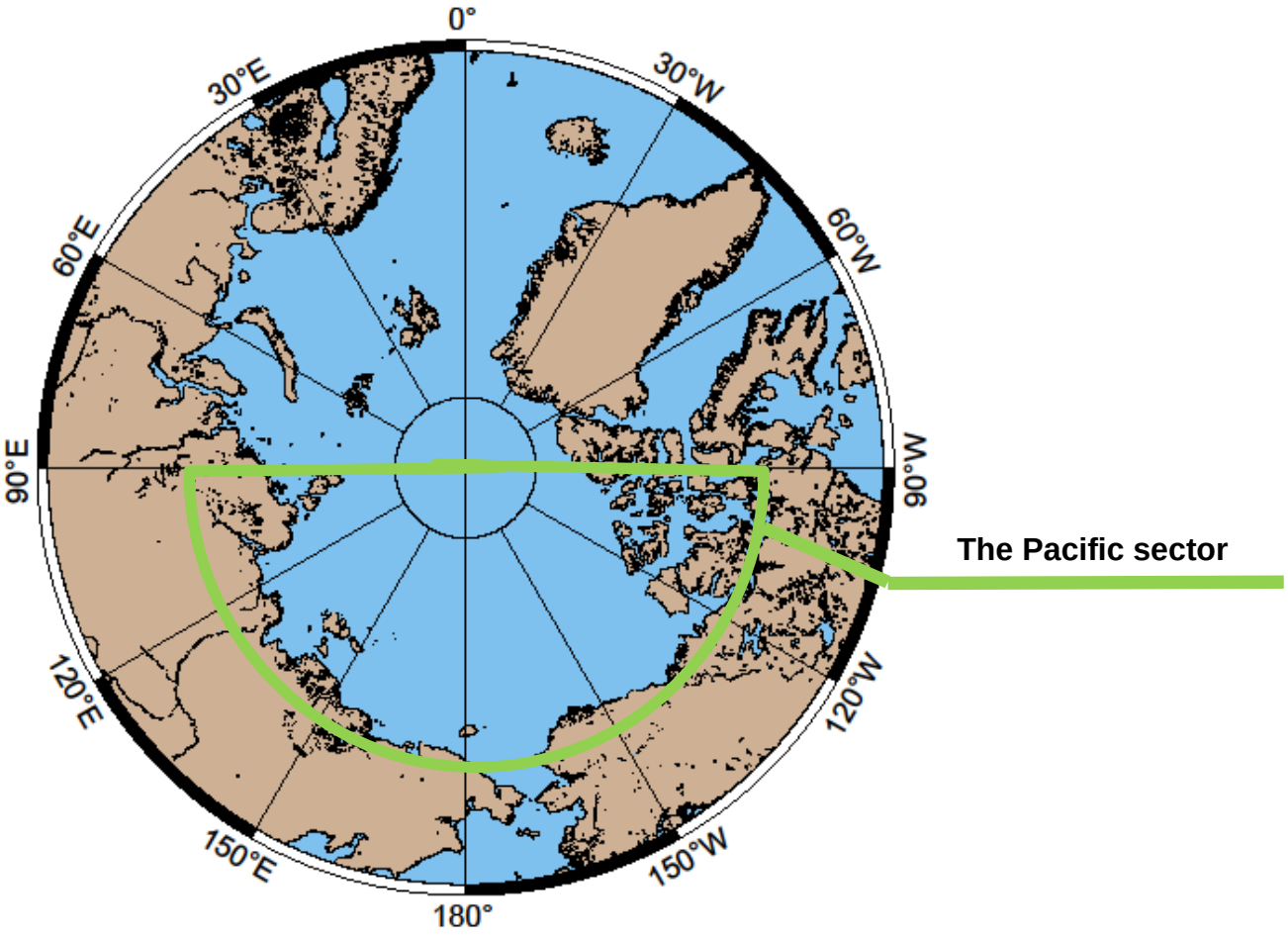

Figure.5 Object domain

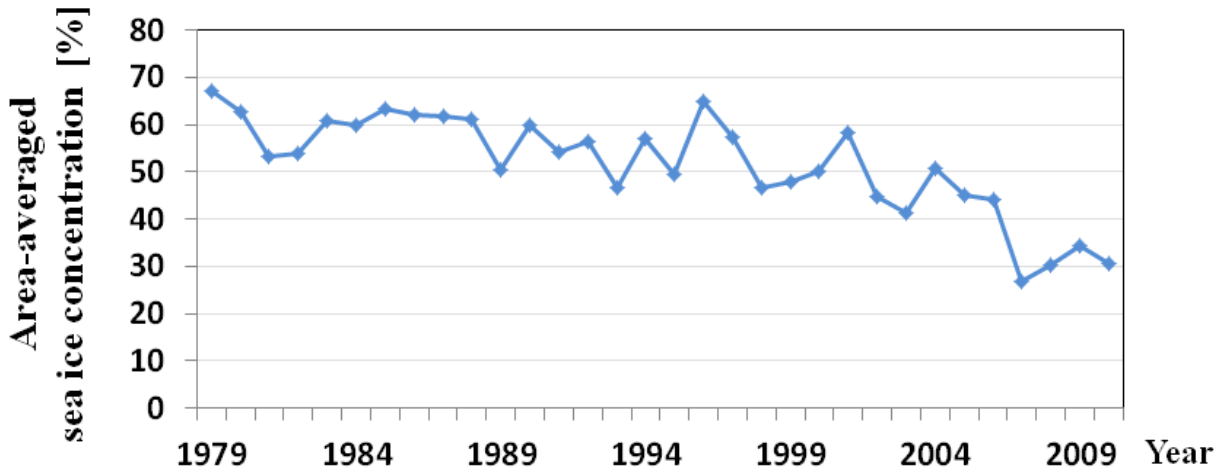

Figure.6 Time series of the minimum value of area-averaged sea-ice concentration in the Pacific sector from 1979 to 2010.

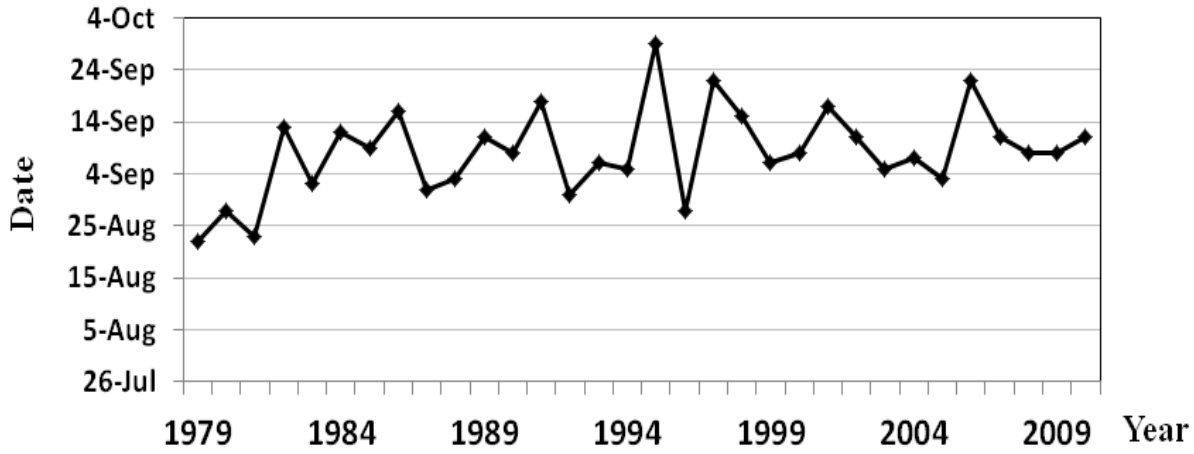

Figure.7 Time series of the date when the sea-ice value is minimum from 1979 to 2010.

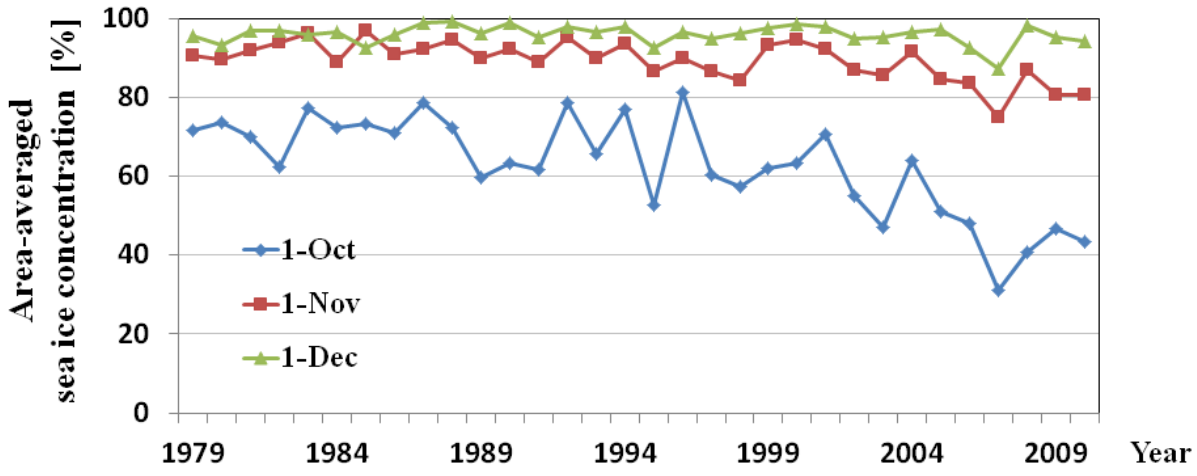

Figure.8　Time series of area-averaged sea-ice concentration at 1st on Oct. (blue line), Nov. (red line) and Dec. (green line) from 1979 to 2010.

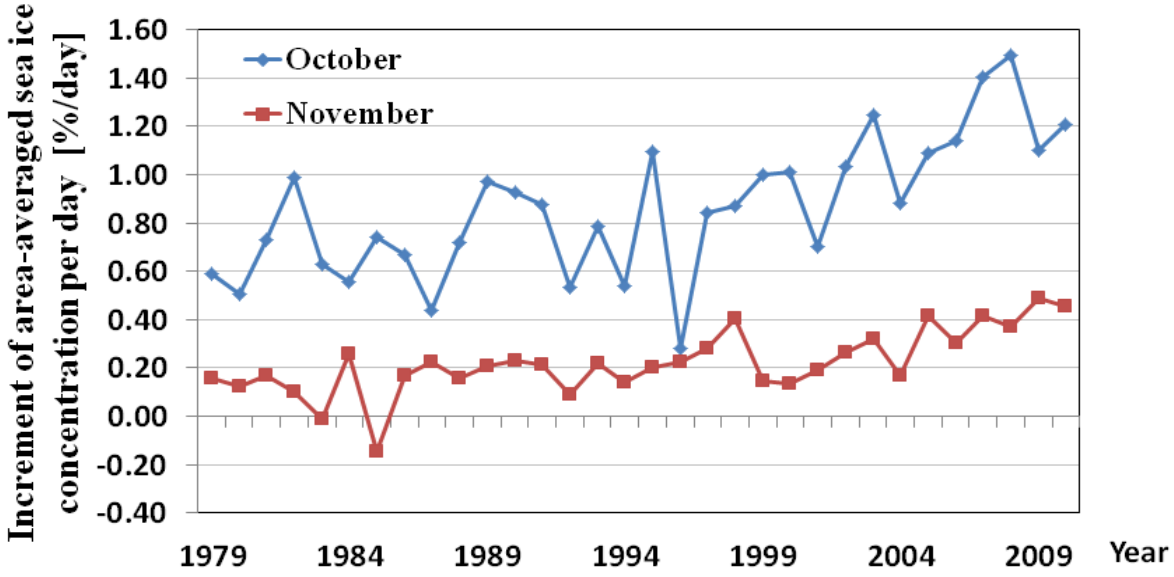

Figure.9 Time series of increment of area-averaged sea-ice concentration per day on Oct. and Nov. from 1979 to 2010.

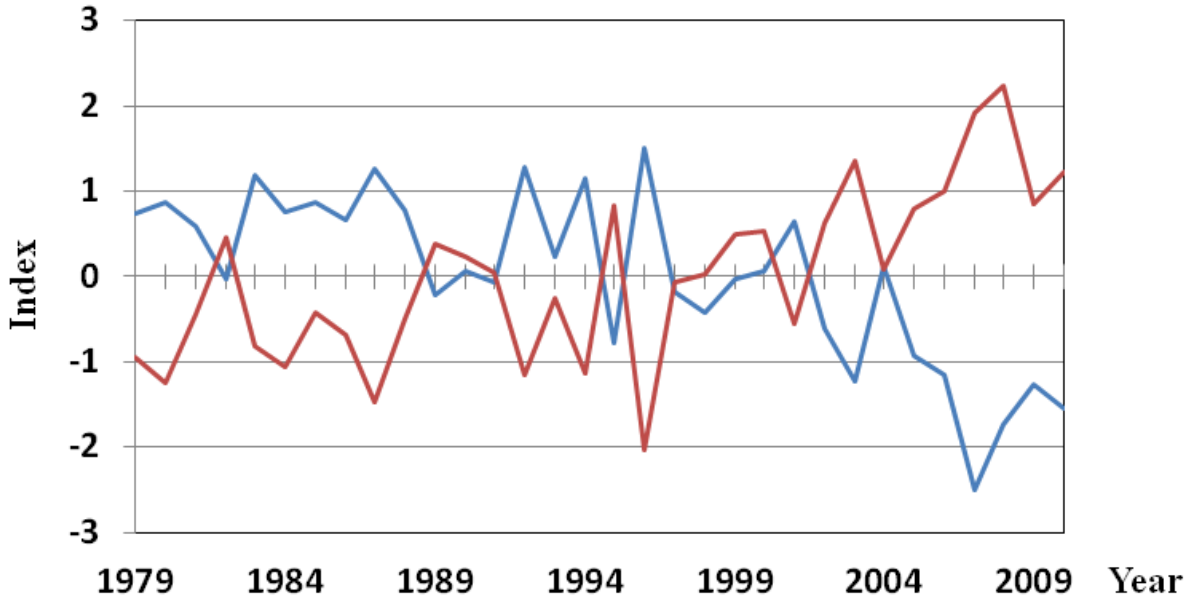

Figure.10 Time series of standardized sea-ice concentration at 1st on October (blue line) and the recovery rate per day on October (red line).

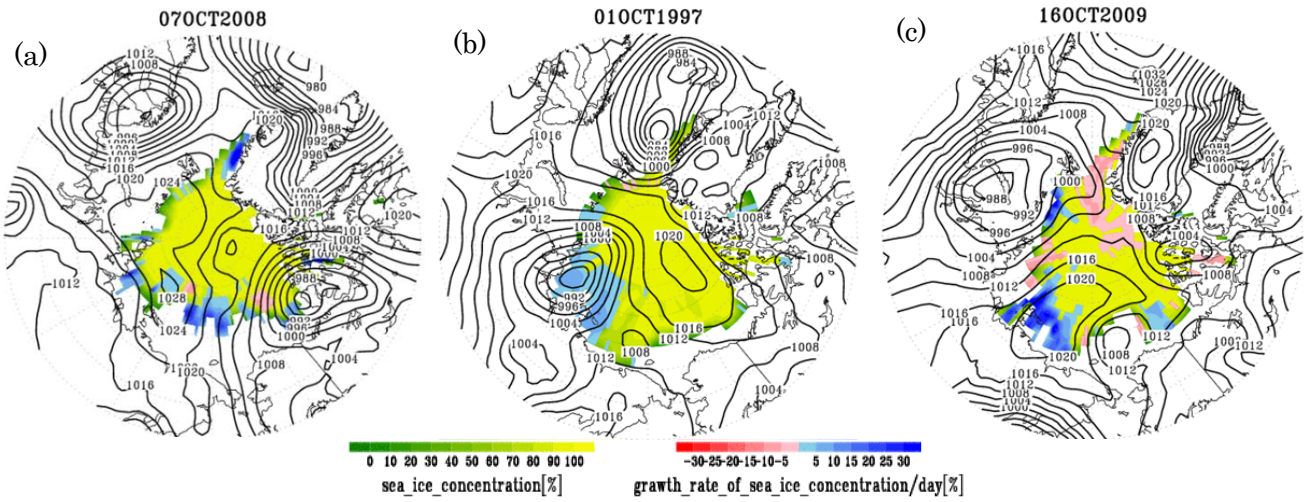

Figure.11 These are maps of which center is north pole. These show sea-ice concentration [%] (sea-ice area is shown in yellow, and ice edge is shown in green), growth rate of sea-ice concentration per day [%/day](decreasing sea ice area is shown as red, and increasing se ice is shown as blue), and sea level pressure [hPa] (contour) at the turning point day. (a) Typical dipole pattern (2008/10/07): a low-pressure system and a high-pressure system are located in pairs around North Pole. (b) Typical single low-pressure system pattern (1997/10/01): a low-pressure system is located over the Laptev Sea or the East Siberian Sea. (c) Typical single high-pressure system pattern (2009/10/16): a high-pressure system is located around North Pole.

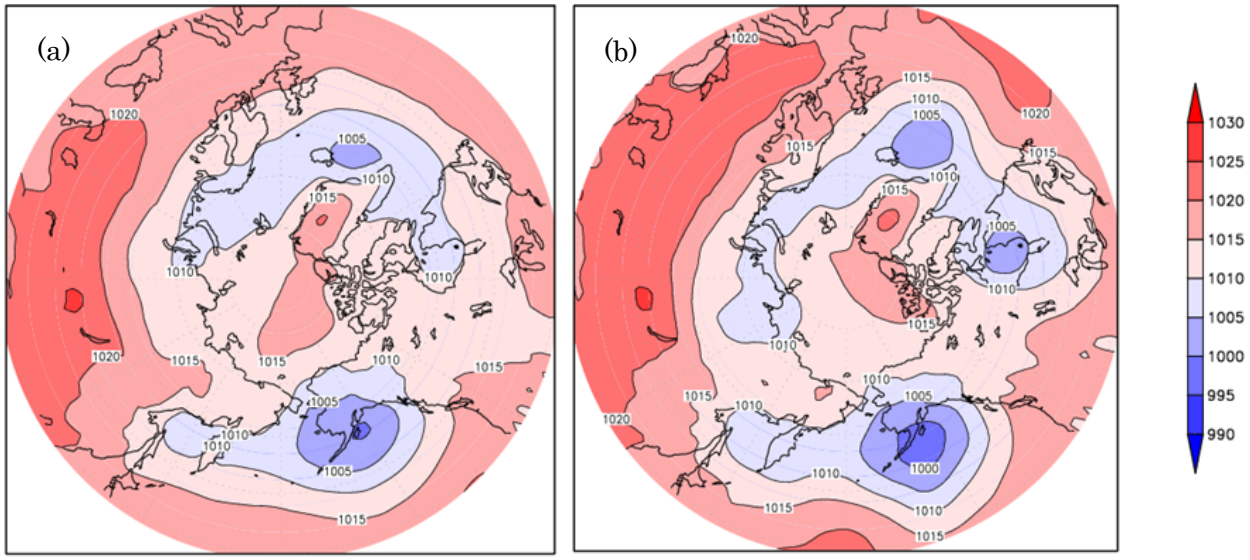

Figure.12　SLP composite [hPa] (a) the recovery rate of sea-ice per day is over 1% (b) the recovery rate of sea-ice per day is over 2%.

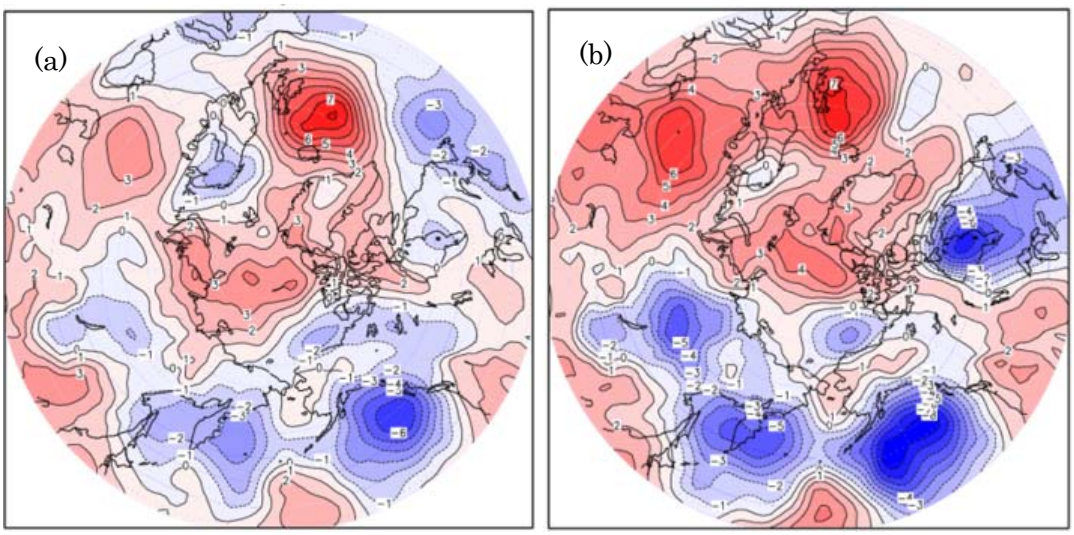

Figure.13　SLP composite anomaly [hPa] (a) the recovery rate of sea-ice per day is over 1% (b) the recovery rate of sea-ice per day is over 2%.

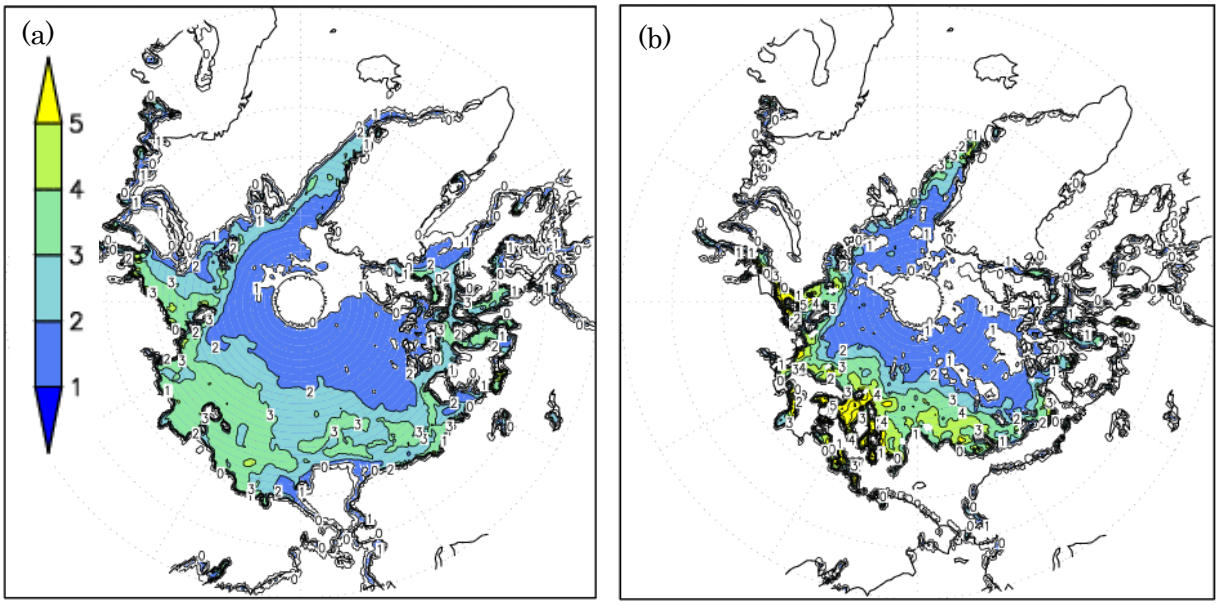

Figure. 14 The composite of PSI recovery rate per day [%/day] (a) the recovery rate of sea-ice per day is over 1% (b) the recovery rate of sea-ice per day is over 2%.

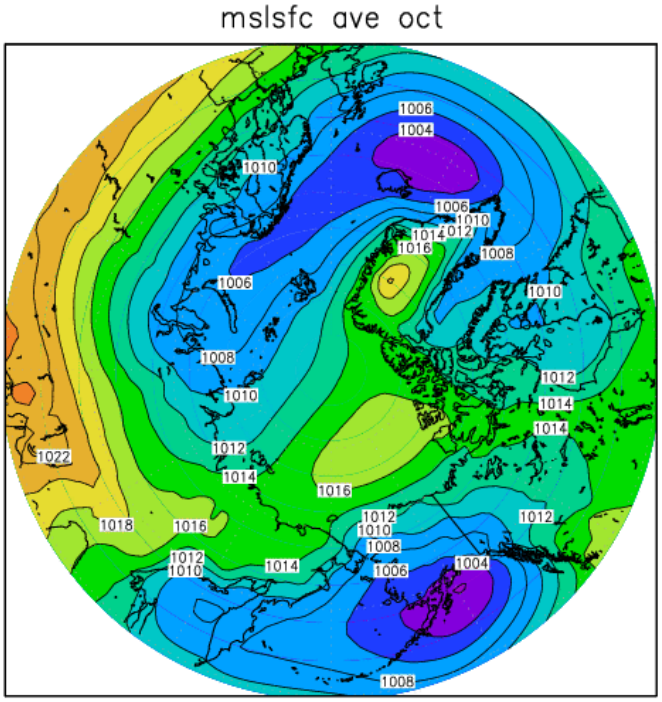

Figure.15 The climate value of SLP on October.

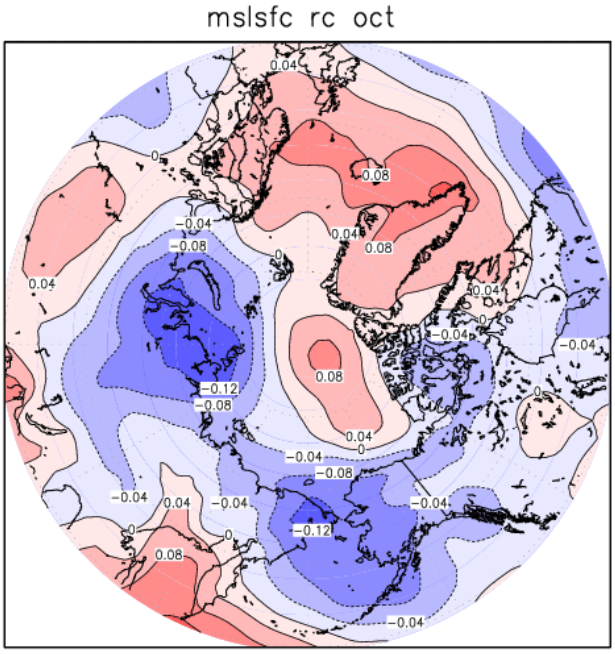

Figure.16 The trend of SLP on October

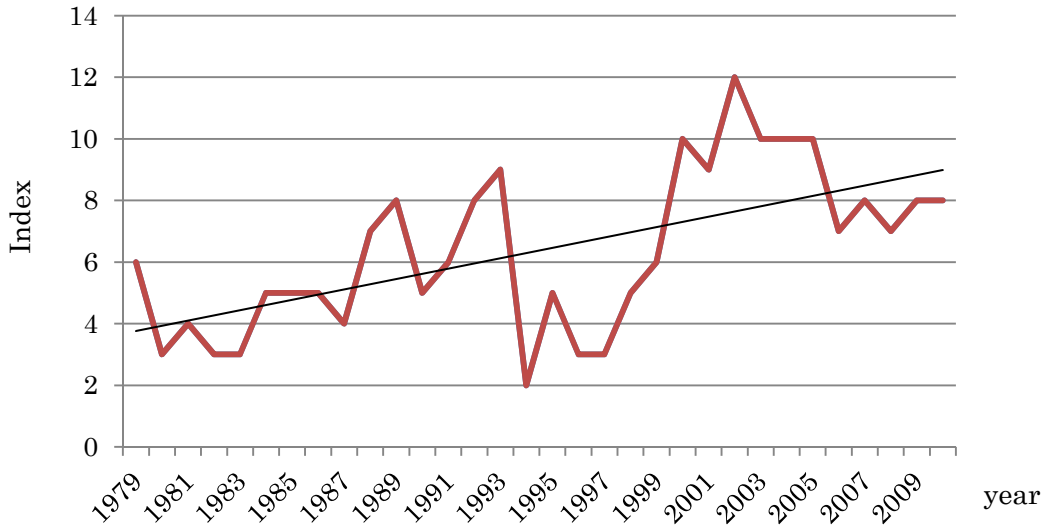

Figure.17 Index of pattern correlation between SLP composite anomalies with daily SLP anomaly.

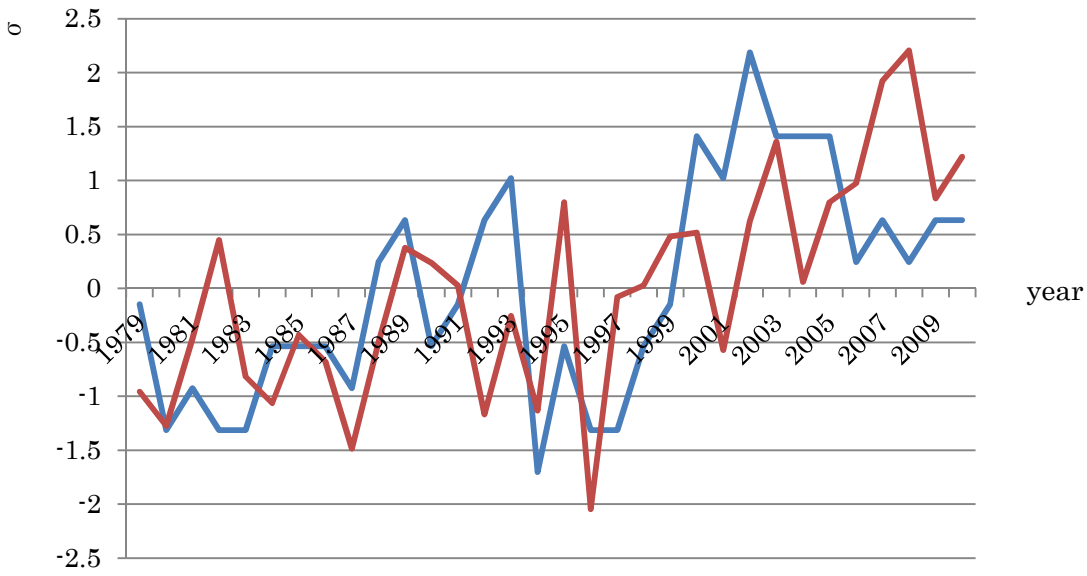

Figure.18 Index of pattern correlation between SLP composite anomalies with daily SLP anomalies on October (blue line) and index of increment of area-averaged sea-ice concentration per day on October (red line).

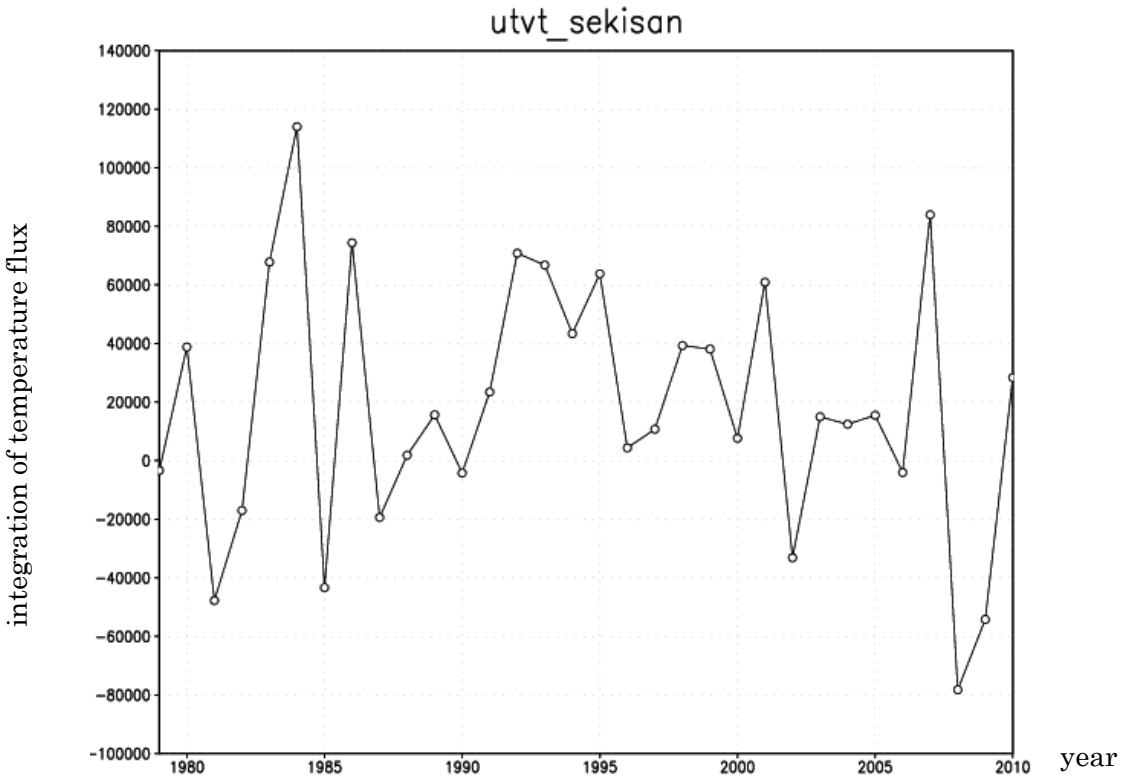

Figure.19 The integration of horizontal temperature flux in the Pacific sector on October from 1979 to 2010.